Soft Matter

PAPER

View Article Online
View Journal

Cite this: DOI: 10.1039/d4sm01027b

Obstacle-enhanced spontaneous oscillation of confined active granules†

Xue Zhang, [a] Yuxin Tian, [a] Ran Ni, [b] Yong Zhu, [c] Luhui Ning, *[de] Peng Liu, *[a] Mingcheng Yang *[fgh] and Ning Zheng *[a]

Received 28th August 2024,
Accepted 31st October 2024

DOI: 10.1039/d4sm01027b

rsc.li/soft-matter-journal

Spontaneous oscillation in particle numbers has been reported recently, in which two chambers connected by a narrow channel are alternately filled and emptied by self-propelled particles. The challenge in realizing the application of this oscillation lies in promotion of the oscillatory periodicity. By placing an asymmetric obstacle at an appropriate position near a channel opening, we can significantly improve the oscillation quality, which approaches the quality of an ideal oscillation. Additionally, we experimentally explore the relationship between the oscillation quality and various system parameters such as the obstacle position. Based on experimental observations, we incorporate a random noise into our previous model and properly reproduce the experimental results. The agreement between theory and experiment uncovers the mechanism of delicate competition between noise and unidirectional particle flow in influencing the oscillation quality. Our findings provide new insights for the optimization of the oscillation quality, expand the conventional rectification capability of the ratchet effect due to the obstacle, and make it possible for spontaneous oscillation to serve as a reliable source for rhythmic signals.

1. Introduction

Due to its non-equilibrium nature, active matter frequently exhibits exceptional collective behaviors that are unprecedented in an equilibrium system. Various behaviors encompass ratcheting effects,[1–4] active crystals,[5–9] giant number fluctuations,[10,11] topological edge flow,[12–15] and spontaneous oscillation.[16–19] Among these behaviors, spontaneous oscillation is a very special and significant type because it is a basic element to understand a universal collective phenomenon – synchronization.[20,21] Its occurrence is recognized as a signature of instability in linearized equations of motion. Additionally, a reliable system capable of generating controllable spontaneous oscillation is a fundamental prerequisite for many potential applications,[22] such as serving as a periodic clock.[18]

Recently, both simulations and experiments have found a novel type of spontaneous oscillation-population or particle number oscillation[23,24] that differs from conventional oscillation in the direction or magnitude of motion of active particles.[16–19,25–27] When a monolayer of artificial active particles is placed in two containers connected by a narrow channel, these particles can alternately fill two chambers, resulting in periodicity in the particle number over time. In addition to its scientific interest and significance, the phenomenon also holds attractive advantages for potential applications. In this scenario, there is no need to preprogramme instructions for the particles to transport cargos. By only constructing a simple geometric structure and endowing the particles with activity, the particles can autonomously accomplish the targeted transportation of materials. Besides, the number of particles during transportation oscillates periodically over time, which can serve as a rhythmic signal for active devices.

However, the oscillation period in previous studies exhibited unsatisfactory quality, even in simulations. Such oscillation with a low periodic quality severely reduces the transportation efficiency, as a notable decrease in the number of transporting particles occurs during flow reversal. And, the resulting

[a] School of Physics, Beijing Institute of Technology, Beijing 100081, China. E-mail: liupeng@bit.edu.cn, ningzheng@bit.edu.cn
[b] School of Chemistry, Chemical Engineering and Biotechnology, Nanyang Technological University, 62 Nanyang Drive, 637459, Singapore
[c] Science and Technology on Electromagnetic Scattering Laboratory, Beijing 100854, China
[d] Beijing Key Laboratory of Optical Detection Technology for Oil and Gas, China University of Petroleum-Beijing, Beijing 102249, China. E-mail: lhningphy@cup.edu.cn
[e] Basic Research Center for Energy Interdisciplinary, College of Science, China University of Petroleum-Beijing, Beijing 102249, China
[f] Beijing National Laboratory for Condensed Matter Physics and Laboratory of Soft Matter Physics, Institute of Physics, Chinese Academy of Sciences, Beijing 100190, China. E-mail: mcyang@iphy.ac.cn
[g] School of Physical Sciences, University of Chinese Academy of Sciences, Beijing 100049, China
[h] Songshan Lake Materials Laboratory, Dongguan, Guangdong 523808, China

† Electronic supplementary information (ESI) available. See DOI: https://doi.org/10.1039/d4sm01027b

periodic signal would be inadequate as a reliable rhythmic source. Even more importantly, the aperiodic oscillation obstructs further exploration into cooperative motion and synchronization of active particles. Apart from the system exhibiting the particle number oscillation, the issue of unsatisfactory oscillation quality is also common in other active systems. The oscillatory periodic signals in these systems often rely on multiple averaging to be extracted, which is particularly prominent in artificial active matter. Consequently, enhancing the oscillation quality in active systems has emerged as a significant and common challenge.

The quality of oscillation periodicity is closely related to the robustness of the unidirectional particle flow in the channel. If the stability of the unidirectional flow can be enhanced, or the noise causing random interruptions in the unidirectional flow can be weakened, it is expected that the oscillation quality will be significantly improved. The key to maintaining the stability of the unidirectional flow lies in promptly guiding active particles into the channel, that is, achieving directional transport of particles towards the channel opening. As is well known, the ratchet effect plays a crucial role in the directed transport of active particles. Among various ratchet structures, obstacles, as an effective and simple means, can rectify the motion of active particles, enabling directed transport in various scenarios.[28–33] Inspired by the distinctive phenomenon in active matter, it seems feasible to exploit the ratchet effect between obstacles and particles to enhance the stability of unidirectional flow, thereby further improving the oscillation quality.

In this article, we present a simple method that effectively addresses this complex problem. We place a specially designed obstacle in front of the channel openings. By adjusting the obstacle's position, we have promoted the oscillation quality – a quantitative measure of the periodicity – to three times its original value, approaching the oscillation quality of an ideal oscillation. Furthermore, we have systematically investigated the dependence of the oscillation quality on the system parameters. According to experimental observations, we introduce noise into the previous model and successfully reproduce the relationship between the oscillation quality, amplitude, frequency, and system parameters. The theoretical and experimental results are generally consistent, and thus reveal its essential mechanism influencing the oscillation quality.

2. Results and discussion

2.1. Experimental results

As shown in Fig. 1, two circular vessels connected by a straight narrow channel are fixed onto an electromagnetic shaker. The asymmetrical dumbbell-shaped particles used in the experiment are composed of a large sphere and a small sphere connected by a rigid rod. The diameter of the large sphere (d_b) is 4 mm, and the diameter of the small sphere (d_s) is 2.5 mm. The mean squared displacement (MSD) of an active granular particle can be found in the ESI.† Vibration-activated granular particles shuttle between two chambers through the

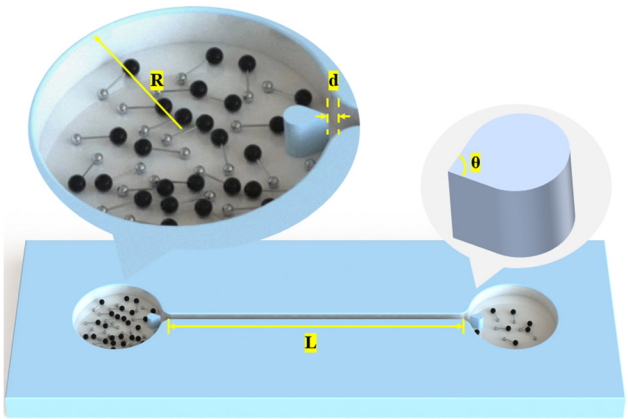

Fig. 1 Schematic diagram of the experimental system (top view) with geometric features. R indicates the radius of the chamber, L the length of the channel, d the distance between the obstacle and the channel opening, and θ the angle of the obstacle tip. The enlarged images show a teardrop-shaped obstacle located at the passageway of each channel.

channel, periodically filling and emptying each one. The experimental system is very similar to the one used in ref. 24. However, in this system, a teardrop-shaped obstacle is placed inside each container, at a distance of d from the channel opening. The obstacle's shape comprises an isosceles triangle and a semicircle with a radius of 3 mm, as shown in the enlarged image of Fig. 1. Experimental videos for conditions with and without obstacles are available in the ESI.†

With the obstacles, the periodicity of the spontaneous population oscillation is notably improved. Fig. 2(a) and (b) illustrate the time evolution of the normalized particle number in one container without/with obstacles, respectively. In comparison, the curve with obstacles in Fig. 2(b) exhibits a more pronounced periodicity. The peaks and troughs along this curve are more evenly spaced, presenting a smoother profile, void of the erratic spikes observed in Fig. 2(a). This suggests that in the system with obstacles, the unidirectional flow of particles in the channel exhibits remarkable robustness and is hardly interrupted. Fig. 3(a) shows the power spectral density (PSD) of the particle number evolution. It is obtained by performing Fourier transform on the time evolution curve, which can identify main frequency components in a fluctuating signal and provide insight into the power distribution of the

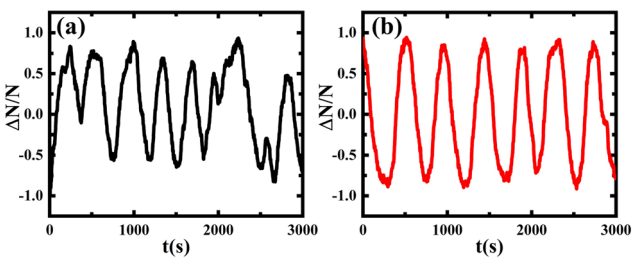

Fig. 2 The time evolution of the fraction of active particles in one container in the oscillatory state, ΔN represents the difference in the number of particles between the two containers. (a) Without obstacles. (b) With obstacles.

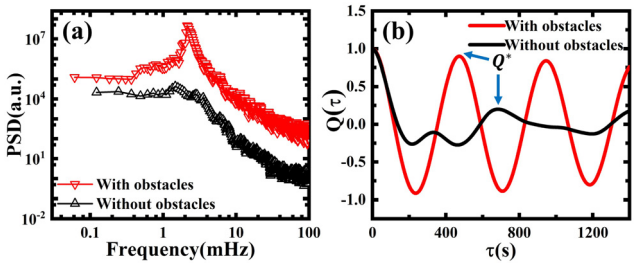

Fig. 3 (a) Power spectrum density (PSD) of the particle number evolution with/without the obstacle. A much sharper peak appears on the curve with the obstacle. (b) Autocorrelation functions for oscillatory curves. The first positive peak Q^* of $Q(\tau)$ characterizes the quality of an oscillation.

signal at different frequencies. The horizontal coordinate corresponding to the peak value represents the oscillation frequency of the system; the more pronounced the peak is, the better the periodicity of the time evolution curve is. It is worth noting that we have also examined the effects of obstacles with various shapes, including circles, triangles and isosceles trapezoids, yet we found that the teardrop-shaped obstacle offers the most significant enhancement in the oscillation quality.

To assess the oscillatory periodicity quantitatively, the autocorrelation function $Q(\tau)$ is applied to evaluate the oscillation quality,[12]

$$Q(\tau) = \frac{\langle S_i(t) S_i(t+\tau) \rangle}{\sigma^2} \quad (1)$$

where $S_i(t) = \frac{\Delta N(t)}{N} - \left\langle \frac{\Delta N(t)}{N} \right\rangle$ is the fluctuation of each data point on the time evolution curve of the particle number; τ represents the time interval; σ is the standard deviation of S_i, and $\langle \cdots \rangle$ indicates averaging over time. The oscillation quality of the spontaneous oscillation is characterized by the first positive peak of the curve $Q(\tau)$, Q^*, also referred to as the oscillation quality factor. The autocorrelation function reflects the self-similarity of the oscillatory curve. For ideal periodic oscillation, the oscillation quality factor is unity.

Under identical conditions, we compared the oscillation quality factors in the presence and absence of the obstacle. To our surprise, the oscillation quality factor is improved from 0.21 to 0.90, representing a substantial increase of more than 300% (see Fig. 3(b)), indicating that it is possible for the spontaneous oscillation to serve as a clock generator for active devices. This type of clock generator has the potential to provide timing signals for the rhythmic movement of soft robots and for programmed microfluidic pumping.[18]

The obstacle plays a crucial role in rectifying active particles near the channel opening, ensuring that they enter the channel along the obstacle's surface in the correct orientation. The obstacle rectification serves two primary functions. Firstly, when the head of the active particle collides with the side of the isosceles triangle of an obstacle, the active particle will have a high probability of sliding into the channel along the obstacle. In contrast, the likelihood of particles entering into the channel drops considerably without the presence of the obstacle, causing in-channel unidirectional flow interruptions and thus resulting in a premature flow reversal. Secondly, the obstacle placed at an appropriate position allows particles to enter the channel with almost 100% probability in the correct posture (*i.e.* the head enters the channel first). Statistical data show that with the obstacle, the probability of particle's head entering the channel is 98.3%, whereas without the obstacle, this probability falls to 91.0% (based on 500 particle entry events). Compared to the second functionality from the obstacle, the first one is more effective in enhancing the stability of the unidirectional flow in the channel. It greatly reduces the probability of random changes in the direction of the particle's motion near the channel opening, thereby significantly improving the oscillation quality. We also analyzed the orientation distribution of particles near the exit under conditions with and without obstacles. Further details can be found in the ESI.†

It should be pointed out that, in the case of granular flow, the size, position, shape, and arrangement of obstacles have a significant impact on the flow rate.[34–36] When positioned appropriately, the obstacle can enhance the flow rate. The improvement of the flow primarily stems from the reduction of the clogging probability of particles at the outlet. More specifically, the obstacle mitigates the packing density and the fluctuation in instantaneous flow rate of particles at the outlet. As a result, the pressure exerted by particles at the outlet is lessened, which disfavors the formation of clogging arches and, in turn, helps to prevent the particle clogging. In contrast, obstacles in the active matter play a role which differs from their functionality in granular flow. Primarily, obstacles in the context of active matter act as rectifiers, regulating the direction of particle's motion.

As previously mentioned, experimental system parameters such as the total number of particles N, the channel length L, and the distance of obstacles from the channel opening d directly affect the oscillation quality. Therefore, we proceeded to investigate how the oscillation quality factor Q^* varies with these parameters, and the results are shown in Fig. 4. Fig. 4(a) shows the relationship between the oscillation quality factor and the total particle number. Basically, as the particle number increases, the oscillation quality factor exhibits a monotonic growth trend. Fig. 4(b) exhibits the dependence of the oscillation quality factor on the channel length. It clearly shows that as the channel length increases, the oscillation quality factor gradually improves until it tends to a plateau when the channel length reaches a certain threshold. In Fig. 4(c), the non-monotonic relationship between the oscillation quality factor and obstacle location is clearly displayed. It is evident that when the obstacle is situated at an optimal position, the oscillation quality factor attains its peak value. Beyond the optimum, the oscillation quality factor experiences a continuous decline until it approximates that of the oscillation without an obstacle ($Q^* = 0.21$).

2.2. Theoretical results

As evidenced by the experimental observations, the primary ingredient for the poor oscillation quality lies in the inadequate

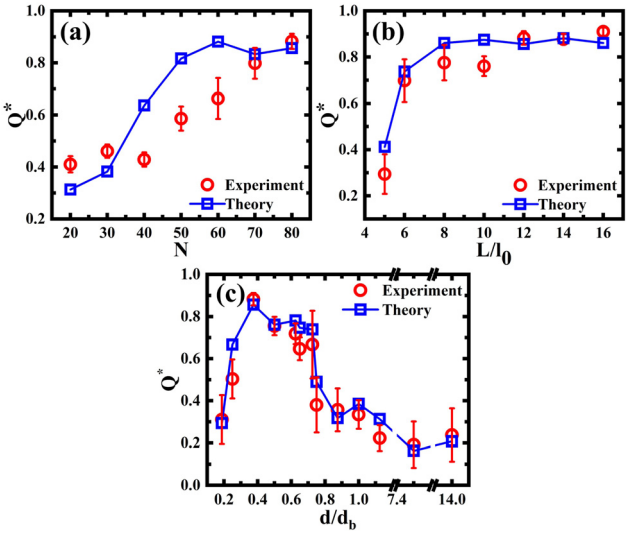

Fig. 4 Comparison of experimental and theoretical results. The oscillation quality factor Q^* as a function of (a) the total particle number N, (b) the channel length L, and (c) the distance d between the obstacle and the channel. L has been normalized by the particle's length l_0, and d has been normalized by the diameter of the large sphere d_b. All figures share common fitting parameters, $a = 5 \times 10^4$ mm and $b = 6.5 \times 10^3$ mm.

robustness of the unidirectional particle flow in the channel. Specifically, if the unidirectional flow of particles shuttling between two chambers is susceptible to be affected by an external noise, the persistence of the flow will be unstable. As such, the unidirectional flow can be disrupted at random, causing a premature reversal in the direction of motion. The significant enhancement of the oscillation quality indicates that we have successfully optimized the robustness of the unidirectional flow. When viewed from another perspective, this essentially implies that we have equivalently mitigated the system noise that hinders the stable existence of the unidirectional flow.

The previous theoretical model, which employed force balance and particle conservation equations, properly reproduced the characteristics of the spontaneous oscillation achieved in experiments.[24] Briefly, the reversal trigger happens, when the force due to the particles from the crowded sink chamber is larger than that from the particles in the unidirectional flow. Specifically, in this model, during the stable unidirectional flow, the channel primarily contains particles from the source chamber. Therefore, it is assumed that the particle number density in the channel, n_c, is the same as that of the source chamber, *i.e.*, $n_c = n_l$. Hence, before the reversal of unidirectional flow, the number of particles in the channel was $N_c = n_c L w = n_l L w$ (where $w = 5$ mm represents the channel width), and the average particle spacing was $\Delta L = L/N_c = 1/n_l w$. When the leading particle in the unidirectional flow enters the sink chamber, a space of length $(\Delta L - l_0)$ is left at the end of the channel near the sink chamber. Subsequently, particles from the sink chamber (moving against the original unidirectional flow) quickly enter the channel and meet the original unidirectional flow at a position $(\Delta L - l_0)/2$ from the end of the sink chamber. Thus, in this scenario, there are $n_h w(\Delta L - l_0)/2$ particles from the sink chamber in the channel. From this, the force balance condition triggering unidirectional flow reversal is formulated.[24] While the model offers valuable insights, it also exhibits notable limitations. Being a deterministic model, it fails to account for stochasticity during the oscillating process, a crucial factor for comprehending the mechanism underlying oscillating quality enhancement. Indeed, large stochastic noise in the system can undermine the robustness of the unidirectional flow, resulting in a random reversal. The random reversal has a direct negative impact on the oscillation quality. To unveil the physical mechanism behind oscillation quality enhancement, we have made appropriate modifications to our earlier model.

Based on the analysis above, we have introduced a noise term into the original model, and the modified equation is written as follows,

$$\frac{n_h w}{2}\left(\frac{1}{n_l w} - l_0\right) = n_l L w - 1 + \chi\xi \tag{2}$$

where ξ is a random variable with a mean of zero and a variance of one, and χ is the noise intensity, which depends on the channel length L, the distance d from the obstacle to the exit, and the total number of particles N. According to experimental observations, as the channel length L increases, the oscillation quality also rises. This suggests that the random noise, which can adversely influence the oscillatory periodicity, diminishes. For the sake of simplicity, we assume $\chi \sim \frac{1}{L}$. Similarly, as the total number of particles N increases, the oscillation quality also gradually elevates, indicating a decline in the noise magnitude. Again, for simplicity, $\chi \sim \frac{1}{N}$. When it comes to the distance d between the obstacle and the channel opening, the situation becomes slightly more complex. When the obstacle is too close to the channel exit, it is more likely to cause clogging of particles at the opening. This, in turn, interrupts the unidirectional flow, and randomly triggers the flow reversal, ultimately being equivalent to an augmentation of the random noise. Conversely, if the obstacle is too far, it loses its rectifying ability to guide active particles into the channel, thereby augmenting the probability of disruptions in the unidirectional flow and a consequent increase in the noise strength. Only when the obstacle is at the optimal position, will the competition between blocking and rectifying effects yield minimal noise which corresponds to the highest oscillation quality. Given the non-monotonic profile between the oscillation quality and the distance d, it can be assumed that $\chi \sim a\left|1 - \frac{d_0}{d}\right| + b$, d_0 is the optimal position measured from the experiment, and a and b are fitting parameters. We consider the total noise as the product of three individual noise terms, which is expressed as follows,

$$\chi(N, L, d) = \left[a\left|1 - \frac{d_0}{d}\right| + b\right]\frac{1}{LN} \tag{3}$$

Combining the conservation equation of total particle number,

$$(n_h + n_l)S + n_l L w = N \tag{4}$$

with S the surface area of a chamber. By numerically solving eqn (2)–(4) together, we can determine the number density n_h and n_l in two chambers at the spontaneous reversal moment of the unidirectional flow. By using the average particle flow rate measured in the experiment, a series of peaks and valleys along the time evolution curve can be obtained. To provide a more precise depiction of how the particle number changes over time, we employ cubic spline interpolation, based on the obtained peak and valley values, to generate a temporal evolution curve of the particle number. After acquiring the evolution curve, we proceed to calculate the oscillation quality factor Q^* for various L, d, and N, by using the autocorrelation function.

Overall, the theoretical results are in semiquantitative and even quantitative agreement with experimental measurements. It is particularly noteworthy that the same fitting parameters, $a = 5 \times 10^4$ mm and $b = 6.5 \times 10^3$ mm, were used consistently across all graphs in Fig. 4, which further reinforces the validity and credibility of the theoretical model. In Fig. 4(a) and (b), it is seen that Q^* rises with an increase in both N and L. Notably, as L continues to grow, Q^* ultimately reaches a plateau. In Fig. 4(c), as d increases, Q^* exhibits a non-monotonic behavior. The presence of an optimal factor indicates that the obstacle's position exerts a dual effect, namely rectifying (negative) and clogging (positive) effect, on the noise strength. Specifically, when the obstacle is placed too close to the channel, it is more likely to cause particles to clog at the opening. This, in turn, interrupts the unidirectional flow, and randomly triggers the flow reversal, ultimately being equivalent to an augmentation of the random noise. In contrast, an obstacle that is situated too far from the channel loses its rectifying capability to steer active particles into the channel, thereby augmenting the probability of disruptions in the unidirectional flow and a consequent increase in the noise strength. Only when the obstacle is located at its optimal location will the delicate competition between the blocking and rectifying effects yield minimal noise which corresponds to the highest oscillation quality. This experimental phenomenon bears some similarity to the observations in granular flow, where the competition between the clog arching and pressure release at the base of the container leads to the existence of an optimal obstacle position at which the flow rate is maximized.[34]

In addition to the oscillation quality, we also compared the average oscillation amplitude $\langle A \rangle$ and frequency f under different conditions of L, d and N. During a complete oscillatory period, the number of particles shuttling between the two containers is $2(n_h - n_l)S$, and the oscillation amplitude directly reads $\langle A \rangle = (n_h - n_l)S/N$, obtained from the calculated n_h and n_l in the model. Fig. 5(a) shows that $\langle A \rangle$ increases with N, when L and d are given. As the number of particles increases, the corresponding random noise diminishes, facilitating the formation of a stable unidirectional flow. Consequently, the probability of the random reversals is suppressed. When N is large, almost all particles can migrate to the sink container with a high number density before the unidirectional flow reverses. Similarly, for a given N and d, as L increases, $\langle A \rangle$ rises until it reaches saturation. This finding once again confirms that a long channel can enhance the stability of the unidirectional flow, thus reducing the influence of random noise, as illustrated in Fig. 5(b). When N and L are fixed, $\langle A \rangle$ increases initially with obstacle distance and then slightly drops, similar to the changing trend of the oscillation quality. The decrease in $\langle A \rangle$ reflects that when the obstacle is situated too near or too far from the channel, the increased random noise enhances the probability of unidirectional flow disruption, preventing part of particles from reaching the sink container and consequently leading to a decrease in $\langle A \rangle$. Under the three kinds of different conditions, the theoretical results are in semiquantitative agreement with experimental measurements. Additionally, using n_h and n_l obtained from the above equations, and the flow rate J in the channel, the oscillating frequency can be calculated through $\frac{1}{f} = T = 2\int_{N_l}^{N_h} \frac{dN'}{J}$, $N_l = n_l S$ and $N_h = n_h S$,[24] as plotted in Fig. 5(d)–(f). The theoretical results are consistent with the experimental measurement, and even an abrupt frequency drop in Fig. 5(f) is qualitatively consistent with the experimental data.

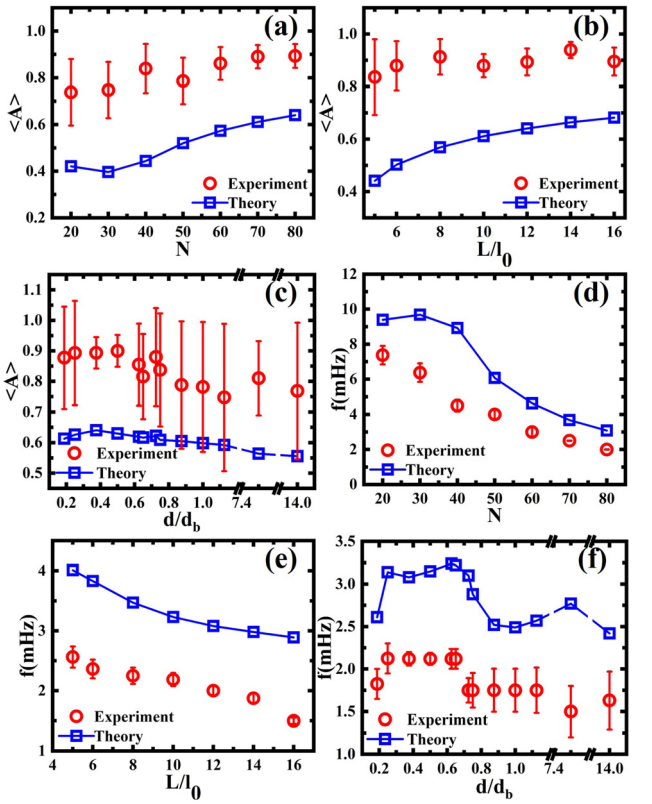

Fig. 5 Comparison of experimental and theoretical results. The average oscillatory amplitude $\langle A \rangle$ and frequency f as a function of (a) and (d) the total particle number, (b) and (e) the channel length, and (c) and (f) the distance of the obstacle from the channel opening.

The modified model properly reproduces the oscillation quality factor, amplitude, and frequency, indicating that it correctly captures the physical mechanism that affects the oscillation quality. The effects of various parameters, such as the obstacle position, channel length, and total particle number, on the oscillation quality may all be equivalently attributed to random noise in the system. The competition between the

random noise and the strength of the unidirectional flow in the channel leads to a probabilistic reversal of this flow. When the noise strength is comparable to that of the unidirectional flow, the stochastic reversal of the flow will occur frequently. The more frequent the random reversal, the lower the self-similarity of the time evolution curve, and hence the lower the oscillation quality. We can lower random noise in various ways, which is equivalent to reducing the probability of the random reversal, to effectively improve the oscillation quality. Nevertheless, there are also limitations in the modified model. For instance, to avoid excessive complexity in the mathematical form of noise, we assumed the simplest possible mathematical form of noise dependence on N, L, and d. While the assumption is reasonable, this phenomenological expression may not be entirely accurate, leading to incomplete quantitative agreement between theoretical and experimental data. Besides, although we have chosen the parameters that have the most significant impact on oscillatory periodicity for modeling, other parameters that affect noise, such as the geometric characteristics of the obstacle, were not taken into account in the model.

3. Conclusions

For the spontaneous oscillation in the vibration-activity system, we have implemented the strategy of introducing an obstacle at the channel opening to enhance its oscillation quality. The experimental results indicate that when the obstacle is appropriately placed, the oscillation quality increases by a factor of three, approaching the oscillation quality of an ideal periodic oscillation. The obstacle effectively directs active particles into the channel, ensuring a stable unidirectional flow and thus preventing the random reversal. This approach expands the conventional rectification capability of the ratchet effect, enriching its functional diversity. Besides, we systematically investigated the dependence of the oscillation quality on the total particle number, the position of the obstacle, and the channel length. With the increase of the total particle number or the channel length, the oscillation quality increases. However, as the obstacle position varies, the oscillation quality exhibits a non-monotonic behavior. Based on the experimental observation and subsequent analysis, we introduced a stochastic noise term into the original theoretical model and phenomenologically established a quantitative relationship between the noise and the total particle number, channel length, and obstacle distance. This modified model properly reproduced the experimental data and revealed the mechanism responsible for the enhancement of the oscillation quality, which is the competition between noise and unidirectional flow leading to the probabilistic reversal of the unidirectional flow. The present experiment of the macroscopic, artificial active matter could stimulate further investigation in biological active systems or microscopic active systems. Whether similar control of the oscillation quality can be realized in these systems remains an interesting open question.

Author contributions

L. N., P. L., M. Y., and N. Z. designed research; X. Z., L. N., P. L., M. Y., and N. Z. performed research; X. Z., Y. T., R. N., Y. Z., L. N., P. L., M. Y., and N. Z. analyzed data; and X. Z., L. N., P. L., M. Y., and N. Z. wrote the paper.

Data availability

All data discussed in the paper are available in the main text and the ESI.†

Conflicts of interest

The authors declare no competing interest.

Acknowledgements

We acknowledge the support from the National Natural Science Foundation of China (Grants No. 12374205, 12304245, 12274448, and T2325027), the Beijing National Laboratory for Condensed Matter Physics (No. 2023BNLCMPKF014), the Science Foundation of China University of Petroleum, Beijing (No. 2462023YJRC031 and 2462024BJRC010), the Academic Research Fund from the Singapore Ministry of Education (RG151/23), and the National Research Foundation, Singapore, under its 29th Competitive Research Program (CRP) Call (Grant No. NRF-CRP29-2022-0002).

Notes and references

1 R. Di Leonardo, L. Angelani, D. DellArciprete, G. Ruocco, V. Iebba, S. Schippa, M. P. Conte, F. Mecarini, F. De Angelis and E. Di Fabrizio, *Proc. Natl. Acad. Sci. U. S. A.*, 2010, **107**, 9541–9545.
2 A. Kaiser, H. Wensink and H. Löwen, *Phys. Rev. Lett.*, 2012, **108**, 268307.
3 P. K. Ghosh, V. R. Misko, F. Marchesoni and F. Nori, *Phys. Rev. Lett.*, 2013, **110**, 268301.
4 G.-h Xu and B.-q Ai, *Soft Matter*, 2021, **17**, 7124–7132.
5 A. M. Menzel, T. Ohta and H. Löwen, *Phys. Rev. E: Stat., Nonlinear, Soft Matter Phys.*, 2014, **89**, 022301.
6 R. Zhang, A. Mozaffari and J. J. de Pablo, *Nat. Rev. Mater.*, 2021, **6**, 437–453.
7 E. Ferrante, A. E. Turgut, M. Dorigo and C. Huepe, *New J. Phys.*, 2013, **15**, 095011.
8 M. James, D. A. Suchla, J. Dunkel and M. Wilczek, *Nat. Commun.*, 2021, **12**, 5630.
9 A. P. Petroff, X.-L. Wu and A. Libchaber, *Phys. Rev. Lett.*, 2015, **114**, 158102.
10 V. Narayan, S. Ramaswamy and N. Menon, *Science*, 2007, **317**, 105–108.

11 S. Dey, D. Das and R. Rajesh, *Phys. Rev. Lett.*, 2012, **108**, 238001.
12 P. Liu, H. Zhu, Y. Zeng, G. Du, L. Ning, D. Wang, K. Chen, Y. Lu, N. Zheng and F. Ye, *et al.*, *Proc. Natl. Acad. Sci. U. S. A.*, 2020, **117**, 11901–11907.
13 X. Yang, C. Ren, K. Cheng and H. Zhang, *Phys. Rev. E*, 2020, **101**, 022603.
14 K. Dasbiswas, K. K. Mandadapu and S. Vaikuntanathan, *Proc. Natl. Acad. Sci. U.S.A.*, 2018, **115**, E9031–E9040.
15 Q. Yang, H. Zhu, P. Liu, R. Liu, Q. Shi, K. Chen, N. Zheng, F. Ye and M. Yang, *Phys. Rev. Lett.*, 2021, **126**, 198001.
16 Y. Sumino, N. Magome, T. Hamada and K. Yoshikawa, *Phys. Rev. Lett.*, 2005, **94**, 068301.
17 Z. Zhang, H. Yuan, Y. Dou, M. O. De La Cruz and K. J. Bishop, *Phys. Rev. Lett.*, 2021, **126**, 258001.
18 S. Liu, S. Shankar, M. C. Marchetti and Y. Wu, *Nature*, 2021, **590**, 80–84.
19 A. E. Hamby, D. K. Vig, S. Safonova and C. W. Wolgemuth, *Sci. Adv.*, 2018, **4**, eaau0125.
20 A. Pikovsky, M. Rosenblum, J. Kurths and R. C. Hilborn, *Synchronization: a universal concept in nonlinear science*, 2002.
21 E. Zheng, M. Brandenbourger, L. Robinet, P. Schall, E. Lerner and C. Coulais, *Phys. Rev. Lett.*, 2023, **130**, 178202.
22 A. Jenkins, *Phys. Rep.*, 2013, **525**, 167–222.
23 M. Paoluzzi, R. Di Leonardo and L. Angelani, *Phys. Rev. Lett.*, 2015, **115**, 188303.
24 W. Li, L. Li, Q. Shi, M. Yang and N. Zheng, *Soft Matter*, 2022, **18**, 5459–5464.
25 Y. Hayashima, M. Nagayama and S. Nakata, *J. Phys. Chem. B*, 2001, **105**, 5353–5357.
26 B. Zhang, B. Hilton, C. Short, A. Souslov and A. Snezhko, *Phys. Rev. Res.*, 2020, **2**, 043225.
27 M. Theillard, R. Alonso-Matilla and D. Saintillan, *Soft Matter*, 2017, **13**, 363–375.
28 H. Li and H. Zhang, *EPL*, 2013, **102**, 50007.
29 L. Angelani, R. Di Leonardo and G. Ruocco, *Phys. Rev. Lett.*, 2009, **102**, 048104.
30 A. Sokolov, M. M. Apodaca, B. A. Grzybowski and I. S. Aranson, *Proc. Natl. Acad. Sci. U. S. A.*, 2010, **107**, 969–974.
31 H.-s Li, C. Wang, Y.-q Ma, C. Xu, N. Zheng and K. Chen, *et al.*, *Soft Matter*, 2017, **13**, 8031–8038.
32 M. Mijalkov and G. Volpe, *Soft Matter*, 2013, **9**, 6376–6381.
33 G. Volpe, I. Buttinoni, D. Vogt, H.-J. Kümmerer and C. Bechinger, *Soft Matter*, 2011, **7**, 8810–8815.
34 I. Zuriguel, A. Janda, A. Garcimartn, C. Lozano, R. Arévalo and D. Maza, *Phys. Rev. Lett.*, 2011, **107**, 278001.
35 A. Garcimartn, J. Pastor, L. Ferrer, J. Ramos, C. Martn-Gómez and I. Zuriguel, *Phys. Rev. E: Stat., Nonlinear, Soft Matter Phys.*, 2015, **91**, 022808.
36 I. Zuriguel, D. R. Parisi, R. C. Hidalgo, C. Lozano, A. Janda, P. A. Gago, J. P. Peralta, L. M. Ferrer, L. A. Pugnaloni and E. Clément, *et al.*, *Sci. Rep.*, 2014, **4**, 7324.